Chronopotentiometry with Programmed Current at a Dropping Mercury Electrode

Jesus Galvez* and Angela Molina

Laboratory of Physical Chemistry, Faculty of Science, University of Murcia, Murcia 239169, Spain

Tomas Perez and M. H. Cordoba

Laboratory of Analytical Chemistry, Faculty of Science, University of Murcia, Murcia 239503, Spain

A theoretical study on the use of the perturbation function $I(t) = I_0t^q$ for chronopotentiometry at the DME is presented. Equations which take into account the sphericity of the electrode are derived both for the potential–time curves and for the transition times. An experimental verification of the theory has been performed with Cd^{2+}, Pb^{2+}, and Zn^{2+} by using the function $I(t) = I_0t$.

Chronopotentiometry with programmed current at stationary electrodes has been known for many years (*1*). However, chronopotentiometry at the DME has received less attention (*2*), in spite of that this electrode has a series of advantages (assurance of a clean and reproducible surface) associated with it. Only Oldham (*3*) and more recently Chow and Ewing (*4*), have presented equations which can be applied to the DME when the expanding plane electrode model (EP) is adopted. In turn, we have shown in a series of recent papers (*2*, *5–7*) in which the EP model was also adopted that DME chronopotentiometry is possible if a current–time function of the form $I(t) = I_0t^{w+1/6}$ ($w \geq 0$) is used. The aim of this paper is to extend the corresponding theory in order to take into account the influence exerted by the sphericity of the electrode (ES model) and to perform an experimental verification of the equations obtained when a function of the form $I(t) = I_0t$ is applied to the DME.

THEORY

Notation and definitions are given in Table I. If we consider the charge-transfer reaction

$$A + ne^- \underset{k_b}{\overset{k_f}{\rightleftharpoons}} B \qquad (I)$$

the expanding sphere boundary value problem is given by

$$\hat{D}_A C_A = \hat{D}_B C_B = 0 \qquad (1)$$

$$\left.\begin{array}{l} t = 0, r \geq r_0 \\ t > 0, r \to \infty \end{array}\right\} C_A = C_A^*, C_B = C_B^* \qquad (2)$$

$t > 0, r = r_0$

$$\frac{I(t)}{nFA(t)} = k_f C_A(0,t) - k_b C_B(0,t) \qquad (3)$$

$$D_A\left(\frac{\partial C_A}{\partial r}\right)_{r=r_0} = -D_B\left(\frac{\partial C_B}{\partial r}\right)_{r=r_0} = \frac{I(t)}{nFA(t)} \qquad (4)$$

where $\hat{D}_i$ is the operator (*8*)

$$\hat{D}_i = \frac{\partial}{\partial t} - D_i\left(\frac{\partial^2}{\partial r^2} + \frac{2}{r}\frac{\partial}{\partial r}\right) + \frac{\zeta^3}{3r^2}\frac{\partial}{\partial r}$$

Table I. Notation and Definitions

k_f, k_b	heterogeneous rate constants of the forward and reverse charge-transfer reaction
k_s ch	apparent heterogeneous rate constant for charge transfer at E°
r	distance from the center of the electrode
r_0	electrode radius at time t
A_0	constant of proportionality of electrode area
$A(t)$	time-dependent electrode area ($=A_0t^{2/3}$)
m	rate of flow of mercury
ζ	$(3m/4\pi d)^{1/3}$
ξ	spherical correction parameter
$E(t)$	time-dependent electrode potential
$I(t)$	time-dependent faradaic current
I_0	constant applied rate of faradaic current increase (eq 7)
Γ	Euler γ function

other definitions are conventional

and double-layer effects have been ignored. In eq 3 k_f and k_b are related to $E(t)$ by

$$k_f = k_s \exp\{-(\alpha nF/RT)\,(E(t) - E^\circ)\} \qquad (5)$$

$$k_b = k_s \exp\{(1-\alpha)(nF/RT)(E(t) - E^\circ)\} \qquad (6)$$

If $I(t)$ has the form

$$I(t) = I_0t^{w+1/6} \qquad (w \geq 0\ (2)) \qquad (7)$$

and we expand C_A and C_B as

$$C_A = \sum_{i,j}\sigma_{i,j}(s_A)\xi_A{}^i\chi^j \qquad (8)$$

$$C_B = \sum_{i,j}\delta_{i,j}(s_B)\xi_B{}^i\chi^j$$

where s_i, ξ_i, and χ are defined by

$$s_i = \sqrt{\frac{7}{12D_it}}\,(r - r_0) \qquad (9)$$

$$\xi_i = \sqrt{\frac{12D_i}{7\zeta^2}}\,t^{1/6}$$

$$\chi = \sqrt{\frac{12}{7D_A}}\,\frac{I_0t^w}{nFA_0C_A^*}$$

we may find the solution of eq 1–4 (see Appendix) so that the surface concentrations of A and B as a function of t are

$$\frac{C_A(0,t)}{C_A^*} = 1 - (1 - f(w)\xi_A)N(w,t) \qquad (10)$$

$$\frac{C_B(0,t)}{C_B^*} = \mu + (1 - f(w)\xi_B)\gamma N(w,t) \qquad (11)$$

0003-2700/84/0356-0887$01.50/0

where

$$f(w) = \frac{1}{22}\left\{7\,(3w+2)p_{6w/7} - \frac{12w(3w+4)}{p_{(6w+1)/7}}\right\} \quad (12)$$

$$N(w,t) = \frac{N_0 t^w}{p_{6w/7}} \quad (13)$$

$$N_0 = \sqrt{\frac{12}{7}}\,\frac{I_0}{nFA_0D_A^{1/2}C_A^*} \quad (14)$$

$$\mu = C_B^*/C_A^* \quad (15)$$

$$\gamma = (D_A/D_B)^{1/2} \quad (16)$$

The transition time, τ, is obtained from eq 10 by making $C_A(0,\tau) = 0$. Thus, for $w > 0$ we find

$$(1 - f(w)\xi_{0,A}\tau^{1/6})\tau^w = \sqrt{\frac{7}{12}}\,\frac{nFA_0D_A^{1/2}C_A^*}{I_0}\,p_{6w/7} \quad (17)$$

where

$$\xi_{0,i} = \sqrt{\frac{12D_i}{7\zeta^2}} \quad (18)$$

It is interesting to show that if $\xi_{0,i} = 0$, eq 17 becomes coincident with that previously derived by Oldham (compare eq 17 with $w = 5/6$ and eq 57b of ref 3 and also with those obtained by Chow and Ewing (see eq 21–23 of ref 4), although the procedure followed by these authors for solving the boundary value problem (they applicated the Laplace transformed method) is different from the one reported in this work.

In turn, the dependence of $E(t)$ on t may be obtained in a dimensionless form making the substitutions

$$\theta(w,t) = \theta_0 t/p_{6w/7}^2 \quad (19)$$

$$\theta_0 = 12k_s^2/7D_A \quad (20)$$

$$\eta(t) = \frac{nF}{RT\ln 10}(E(t) - E^\circ) \quad (21)$$

$$N_i^*(w,t) = (1 - f(w)\xi_{0,i}t^{1/6})N(w,t) \quad (22)$$

and introducing eq 10–11 in eq 3

$$(\theta(w,t))^{-1/2}N(w,t)10^{\alpha\eta(t)} = 1 - N_A^*(w,t) - (\mu + \gamma N_B^*(w,t))10^{\eta(t)} \quad (23)$$

If $k_s >> 1$ (Nernstian behavior) eq 23 becomes

$$\eta(t) = \log\frac{1 - N_A^*(w,t)}{\mu + \gamma N_B^*(w,t)} \quad (24)$$

When $\mu = 0$, we may combine eq 17 and 24, and so this last equation may be rewritten as

$$E(t) = E^\circ - \frac{RT}{nF}\ln\frac{g_A(\tau)}{\gamma g_B(t)} + \frac{RT}{nF}\ln\left\{\left(\frac{\tau}{t}\right)^w - \frac{g_A(t)}{g_B(\tau)}\right\} \quad (25)$$

where

$$g_i(t) = 1 - f(w)\xi_i \quad (26)$$

If $\xi_i = 0$, eq 25 is simplified to

$$E(t) = E_{1/2} + \frac{RT}{nF}\ln\left\{\left(\frac{\tau}{t}\right)^w - 1\right\} \quad (27)$$

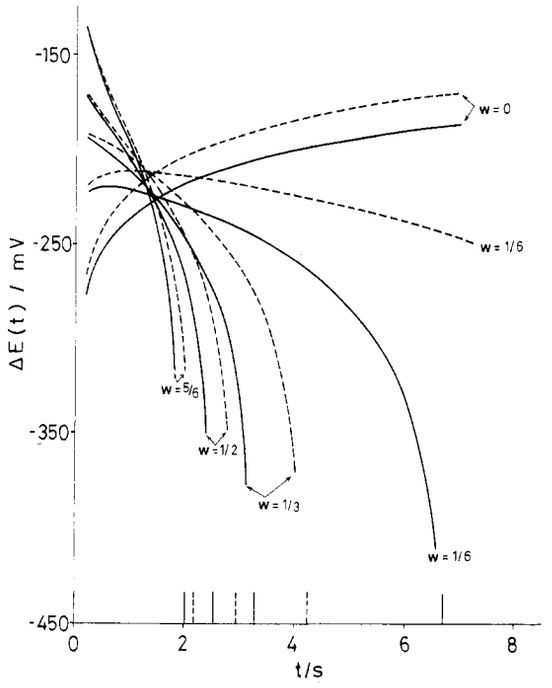

Figure 1. Dependence of $\Delta E(t)$ on t: $\theta_0 = 20\ s^{-1}$; $N_0 = 0.9\ s^{-w}$; $n = 1$; $T = 298$ K; $\mu = 0$; $\gamma = 1$; $\xi_{0,A}$ ($s^{-1/6}$) (---) 0.1, (—) 0.0; w values shown on the curves. The dashed and full lines on the t axis show, respectively, the τ values for the ES and EP models.

From this equation it is readily shown that the t value for which $E(t) = E_{1/2}$, i.e., $t_{1/2}$, is given by

$$t_{1/2} = \tau/2^{1/w} \quad (28)$$

If $k_s << 1$ (totally irreversible process) eq 23 becomes

$$\eta(t) = \log\frac{1 - N_A^*(w,t)}{(\theta(w,t))^{-1/2}N(w,t)} \quad (29)$$

EXPERIMENTAL SECTION

The chronopotentiograms were obtained with an AMEL multipurpose unit, Model 563, equipped with a 551 potentiostat, a 566 function generator, and a 862/D recorder. This equipment allows the application of the function $I(t) = I_0 t$ to the DME for different values of I_0. The electrode reference was SCE and the measurements were performed at 25 °C. Oxygen was removed from the cell by using purified nitrogen. All chemicals used were Analytical Reagent grade and the water was twice distilled.

RESULTS AND DISCUSSION

Dependence of $E(t)$ on θ_0 is similar to that previously described for the EP model (2). Thus, if $0.2 < \theta_0 < 2000\ s^{-1}$ the process (I) is quasi-reversible and eq 23 cannot be simplified. In turn, for θ_0 values greater than $2000\ s^{-1}$ the process may be considered as reversible and eq 24 is applied. Finally, if $\theta_0 < 0.2\ s^{-1}$, the process behaves as totally irreversible and $E(t)$ values computed with eq 29 show good agreement with those computed from eq 23. In Figure 1 we have graphically represented $\Delta E(t)$ ($=E(t) - E^\circ$) vs. t for $\theta_0 = 20\ s^{-1}$, $\xi_{0,A} = 0.1\ s^{-1/6}$, $N_0 = 0.9\ s^{-w}$, and different values of w. By comparison we have also included the corresponding curves for the EP model. Note that the effect exerted by the sphericity of the electrode increases as t becomes greater. In addition, for a given value of t the effect of sphericity also increases if w is lowered and so, if τ values are computed from eq 17 with $\xi_{0,A} = 0$, the deviations for $0 < w < 1/3$ are so great that the EP model is not valid under these conditions. However, if the E/t curves are normalized, i.e., if we plot $E(t)$ vs. t/τ (see Table II) the influence of the electrode curvature is strongly decreased (this situation is analogous to that previously described for the I/E curves in dc polarography (9)). Hence, if absolute values of

Table II. Dependence of $\Delta E(t)$ on t/τ

t/τ	$\Delta E(t)$/mV (I)	$\Delta E(t)$/mV (II)
0.1	−32.91	−32.06
0.2	−42.48	−41.25
0.3	−50.56	−49.18
0.4	−58.32	−56.89
0.5	−66.36	−64.94
0.6	−75.30	−73.96
0.7	−86.03	−84.85
0.8	−100.48	−99.60
0.9	−124.90	−124.73

[a] Normalized E/t curves for $w = 1/6$ and $\xi_{0,A}$ s$^{-1/6}$ = (I) 0.1; (II) 0.0. Other conditions are given in Figure 1.

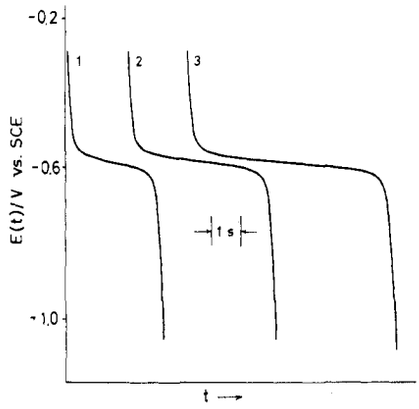

Figure 2. Potential–time curves for Cd(II): C_{NaNO_3} = 0.2 M; m = 0.907 mg·s^{-1}; I_0 = 1 μA·s^{-1}; C_A* (mM) (1) 0.4411, (2) 0.6616, (3) 0.8822.

τ are necessary, they must be computed from eq 17 taking into account the curvature of the electrode (in particular if $w < 1/3$). Conversely, the electrode model is not so critical for the analysis of normalized E/t curves.

Experimental Results. As mentioned above, the AMEL multipurpose unit 563 allows the application of the perturbation function $I(t) = I_0 t$ to the electrode for different values of I_0. Hence, the equations derived above can be used by making $w = 5/6$. Thus, e.g., eq 17 can be rewritten in normal polarographic units (m, mg·s^{-1}; D_A, cm^2·s^{-1}; C_A*, mM; I_0, μA·s^{-1}) at 25 °C as

$$\left(1 - \frac{28.2 D_A^{1/2} \tau^{1/6}}{m^{1/3}}\right) \tau^{5/6} = \frac{1010.6 n m^{2/3} D_A^{1/2} C_A^*}{I_0} \quad (30)$$

We have obtained a great number of chronopotentiograms for the species Cd^{2+}, Pb^{2+}, and Zn^{2+} by using different values of I_0 and C_A*. In all cases, and due to the clean and reproducible surface of the DME, the E/t curves are also perfectly reproducible. An example of the chronopotentiograms obtained for Cd^{2+} is shown in Figure 2.

On the other hand, the transition times obtained from these plots have been compared with those computed from eq 30 and the results are shown in Tables III–V (the corresponding D_A values have been calculated in our experimental conditions from polarographic measurements by using Ilkovic's equation). Note the excellent agreement between both values which confirms the validity of eq 30.

In addition, analyses of these chronopotentiograms have been performed with eq 27. As expected, deviations with eq 25 are small because $g_A(t)/g_A(\tau) \simeq 1$. Thus, e.g., for Pb^{2+} the plot of $E(t)$ vs. log $\{(\tau/t)^{5/6} - 1\}$ is practically linear (r = 0.999 96), with a slope equal to 0.0298 which is in excellent agreement with the theoretical value. In turn, the $t_{1/2}$ value is given by (see eq 28)

$$t_{1/2} = 0.435\tau \quad (31)$$

Table III. Theoretical and Experimental Transition Times for the Reduction of Cd(II) at 25 °C[a]

C_A*, mM	I_0, μA·s^{-1}	τ_{calcd}, s	τ_{exptl}, s
1.1490	2	3.86	3.86
0.9189	4	1.26	1.25
0.9189	2	2.94	2.93
0.8822	1	6.54	6.55
0.6892	2	2.07	2.06
0.6616	1	4.59	4.60
0.4411	1	2.80	2.80
0.2205	1	1.20	1.20
0.2205	0.4	3.67	3.67
0.1103	0.4	1.57	1.60
0.1103	0.2	3.68	3.68
0.0551	0.2	1.57	1.59
0.0551	0.1	3.67	3.66

[a] Comparison of the τ values computed from eq 30 and those obtained from E/t curves: C_{NaNO_3} = 0.2 M, D_A = 6.6 × 10^{-6} cm^2·s^{-1}. m = 0.907 mg·s^{-1}.

Table IV. Theoretical and Experimental Transition Times for the Reduction of Zn(II) at 25 °C[a]

C_A*, mM	I_0, μA·s^{-1}	τ_{calcd}, s	τ_{exptl}, s
1.5220	4	2.29	2.34
1.2180	4	1.74	1.76
1.2180	2	4.06	4.04
0.9135	4	1.23	1.28
0.9135	2	2.86	2.80
0.6088	2	1.74	1.69
0.5850	1	3.87	3.85
0.2923	1	1.65	1.57
0.1461	0.4	2.17	2.09
0.1461	0.2	5.08	5.07

[a] Comparison of the τ values computed from eq 30 and those obtained from E/t curves: C_{NaNO_3} = 0.2 M, D_A = 6.36 × 10^{-6} cm^2·s^{-1}. m = 0.912 mg·s^{-1}.

Table V. Theoretical and Experimental Transition Times for the Reduction of Pb(II) at 25 °C[a]

C_A*, mM	I_0, μA·s^{-1}	τ_{calcd}, s	τ_{exptl}, s
0.8239	4	1.31	1.32
0.8239	2	3.06	3.06
0.6179	2	2.15	2.14
0.5932	1	4.79	4.80
0.3955	1	2.91	2.95
0.1977	1	1.25	1.30
0.0989	0.4	1.64	1.69
0.0989	0.2	3.83	4.02
0.0494	0.2	1.64	1.70
0.0494	0.1	3.83	4.01

[a] Comparison of the τ values computed from eq 30 and those obtained from E/t curves: C_{NaNO_3} = 0.2 M, D_A = 8.35 × 10^{-6} cm^2·s^{-1}, m = 0.926 mg·s^{-1}.

We have found from the corresponding E/t curve that $E(t)$ for $t = t_{1/2}$ is equal to −383 mV, while the value obtained from the intercept is −386 mV. These results are also in good agreement with literatura data (*10*), and they are, therefore, an additional confirmation of the theory above exposed.

Analytical Applications. According to eq 30 the relationship between $\tau^{5/6}$ and C_A* is not linear. However, from a practical point of view (τ varying between 1 and 6 s) $g_A(\tau)$ is almost constant (for $\xi_{0,A}$ = 0.1 s$^{-1/6}$, $g_A(1)$ = 0.9439, and $g_A(6)$ = 0.9244). Under these conditions a plot of $I_0\tau^{5/6}$ vs. C_A* gives a straight line which is useful for analytical purposes. So, the equation

$$I_0\tau^{5/6} = KC \quad (32)$$

has been used for analytical determination of metallic ions,

Zn^{2+}, Pb^{2+}, and Cd^{2+} in concentrations ranging from 5×10^{-5} to 2×10^{-3} M with excellent analytical results (thus, e.g., the coefficient of variation for ten successive determinations of Cd^{2+} at the 10^{-4} M level was ±0.8%). Hence, chronopotentiometry with a linear sweep of current at the DME appears to be a method with great analytical possibilities and has the additional advantage over classical chronopotentiometry at stationary electrodes with constant current of a clean and reproducible surface electrode.

Finally, it is also interesting to show that eq 17 hints at the advantage of using the function $I(t) = I_0 t^{7/6}$ for DME chronopotentiometry because in this case the relationship between τ and C is linear.

APPENDIX

In eq 8 the $\sigma_{i,j}(s_A)$ functions are obtained by using the dimensionless parameter method previously described (*2*, *5*–*7*). Thus, we have

$$\sigma_{0,0}(s_A) = C_A^* \tag{A1}$$

$$\sigma_{0,1}(s_A) = -\frac{C_A^*}{p_{6w/7}} \psi_{6w/7}$$

$$\sigma_{0,j}(s_A) = 0; \quad j \geq 2$$

and

$$\sigma_{1,0}(s_A) = 0 \tag{A2}$$

$$\sigma_{1,1}(s_A) = \beta_1\psi_{(6w-21)/7} + \beta_2\psi_{(6w-7)/7} + \beta_3\psi_{(6w+7)/7} + \beta_4\psi_{6w/7}$$

where

$$p_j = \frac{2\Gamma(1 + j/2)}{\Gamma(1 + j/2)} \tag{A3}$$

and

$$\beta_1 = -\frac{3(6w - 7)}{27} C_A^* \tag{A4}$$

$$\beta_2 = \frac{9w + 7}{14} C_A^*$$

$$\beta_3 = \frac{3w}{7} C_A^*$$

$$\beta_4 = -\frac{6w(3w + 4)}{11 p_{6w/7} p_{(6w+1)/7}} C_A^*$$

and the ψ's are the functions defined by Koutecký (*11*). In turn, the $\delta_{i,j}(s_B)$ are obtained in an analogous way. Finally, from eq A1–A4 and taking into account that $\psi_i(0) = 1$ (*11*), we find eq 10.

Registry No. Cd, 7440-43-9; Pb, 7439-92-1; Zn, 7440-66-6; mercury, 7439-97-6.

LITERATURE CITED

(1) Bard, Allen J.; Faulkner, Larry R. "Electrochemical Methods", Wiley: New York, 1980; Chapter 7 and references therein.
(2) Galvez, J. *J. Electroanal. Chem.* **1982**, *132*, 15.
(3) Oldham, Keith B. *Anal. Chem.* **1969**, *41*, 936.
(4) Chow, Li Hang; Ewing, Galen W. *Anal. Chem.* **1979**, *51*, 322.
(5) Galvez, J.; Molina, A. *J. Electroanal. Chem.* **1983**, *146*, 221.
(6) Galvez, J.; Saura, R. *J. Electroanal. Chem.* **1983**, *146*, 233.
(7) Galvez, J.; Fuente, T.; Molina, A.; Saura, R. *J. Electroanal. Chem.* **1983**, *146*, 243.
(8) Heyrovsky, J.; Kuta, J. "Principles of Polarography"; Academic Press: New York, 1966; p 92.
(9) Galvez, J.; Molina, A.; Fuente, T. *J. Electroanal. Chem.* **1980**, *107*, 217.
(10) Heyrovsky, J.; Kuta, J. "Principles of Polarography"; Academic Press: New York, 1966; p 542.
(11) Koutecký, J. *Czech. J. Phys.* **1953**, *2*, 50.

RECEIVED for review September 29, 1983. Accepted December 30, 1983. We thank the Comision Asesora de Investigación Científica y Técnica for supporting this study (Projects 321/81 and 854/81).

Spatial Resolution of Electrode Heterogeneity Using Iontophoresis

Royce C. Engstrom

Department of Chemistry, University of South Dakota, Vermillion, South Dakota 57069

The physiological technique of iontophoresis has been adapted to the study of microscopic heterogeneity on solid electrode surfaces. Micropipets having tip diameters of less than 1 μm were filled with a solution of potassium ferrocyanide and positioned over solid working electrode surfaces with a micropositioning device. Electrophoretic ejection of ferrocyanide ions was made onto a localized area of an electrode poised at 0.5 V vs. SCE. Electrochemical reaction of ferrocyanide resulted in a transient Faradaic current, the amplitude of which was taken as a measure of the microscopically local electrode activity. The characteristics of the technique were studied with platinum microelectrodes and epoxy-impregnated reticulated vitreous carbon electrodes. Active regions as small as 10 μm could be detected and two-dimensional mapping of individual active regions was accomplished with a spatial resolution of 10 μm.

It is recognized that solid electrodes can present heterogeneous surfaces with respect to electrochemical activity. For example, heterogeneity on an atomic level might arise from crystal defects or the presence of foreign adatoms. On a microscopic level or larger, heterogeneity might arise from adsorption processes, the presence of surface oxides, surface topography, microcrystallite orientation, or even deliberate electrode design. The first reports on the subject of electrode heterogeneity (*1*, *2*) recognized that deviations from expected electrochemical behavior could result from heterogeneity, and the extent of deviation depended on the sizes of active and inactive regions compared to the dimensions of the diffusion layer. Theoretical treatments of electrode heterogeneity have appeared (*3*–*8*) and attempt to explain the effects of heterogeneity on rotated-disk voltammetry, chronopotentiometry, chronoamperometry, linear potential sweep voltammetry, and cyclic voltammetry. In some cases, the theories have been tested through the use of model heterogeneous electrodes (*4*, *6*, *7*, *9*–*12*).

The theoretical treatments have been used to obtain estimates of the dimensions of heterogeneities at solid electrodes. Measuring the rotation-rate dependence of limiting current, Landsberg and Thiele estimated that their carbon paste

0003-2700/84/0356-0890$01.50/0